Human Molecular Genetics, 2004, Vol. 13, No. 11 ***1171–1181***
DOI: 10.1093/hmg/ddh124
Advance Access published on March 31, 2004

Foxl2 disruption causes mouse ovarian failure by pervasive blockage of follicle development

Manuela Uda[1,2,†], Chris Ottolenghi[1,†], Laura Crisponi[2,†], Jose Elias Garcia[1], Manila Deiana[2], Wendy Kimber[1], Antonino Forabosco[3], Antonio Cao[2], David Schlessinger[1] and Giuseppe Pilia[2,*]

[1]Laboratory of Genetics, National Institute on Aging, Baltimore, MD 21224, USA, [2]Istituto di Neurogenetica e Neurofarmacologia, Consiglio Nazionale delle Ricerche, c/o Ospedale Microcitemico, Via Jenner s/n, Cagliari 09100, Italy and [3]Medical Genetics, Department of Mother and Child, University of Modena and Reggio-Emilia, Policlínico, Via del Pozzo 71, Modena 41100, Italy

Received February 16, 2004; Revised and Accepted March 23, 2004

***FOXL2* mutations cause gonadal dysgenesis or premature ovarian failure (POF) in women, as well as eyelid/forehead dysmorphology in both sexes (the 'blepharophimosis–ptosis–epicanthus inversus syndrome', BPES). Here we report that mice lacking *Foxl2* recapitulate relevant features of human BPES: males and females are small and show distinctive craniofacial morphology with upper eyelids absent. Furthermore, in mice as in humans, sterility is confined to females. Features of *Foxl2* null animals point toward a new mechanism of POF, with all major somatic cell lineages failing to develop around growing oocytes from the time of primordial follicle formation. *Foxl2* disruption thus provides a model for histogenesis and reproductive competence of the ovary.**

INTRODUCTION

Premature ovarian failure (POF) is a common condition, affecting 1–3% of all women, in which incomplete menarche or early menopause could result from inadequate formation or maintenance of the pool of ovarian follicles (ovarian dysgenesis). Ovarian organogenesis starts with the formation of the sexually indifferent gonadal anlage, followed by sex differentiation, with the formation of the primitive ovary. Finally with 'definitive histogenesis' (1), oogonia enter meiosis and oocytes are incorporated into primordial follicles. The perinatal pool of primordial follicles, which later grow and mature, is established by a poorly understood mechanism whereby oocyte nests are coordinately intercalated by somatic cells and fragment into single follicles (1–4). Human X monosomy (5) and several mouse mutants [notably c-*kit* and the c-*kit* ligand/*Steel* (reviewed in 6), *Gcd* (7), *Fig-alpha* (8)] showed that oocyte defects at various developmental stages reduced the number of primordial follicles or totally prevented their formation. More disruptive effects on perinatal ovary differentiation [e.g. *Wnt4* (9), *TrkB* (10)] have been difficult to interpret. Consequently, studies of gonadal dysgenesis in human and animal models have provided little information about the mechanism of primordial follicle formation (11).

The finding that blepharophimosis–ptosis–epicanthus inversus syndrome BPES (OMIM 110100, http://www.ncbi.nlm.nih.gov/entrez/query.fcgi?db = OMIM), a syndrome associated with POF, is caused by heterozygous mutations in *FOXL2*, a gene encoding a forkhead transcription factor (12), provided a possible entry point to the study of ovarian dysgenesis. Here, based on findings in a knockout mouse, we show that *Foxl2* is a selective determinant of perinatal ovarian histogenesis with a central role in primordial follicle formation.

RESULTS

To elucidate anomalies associated with *Foxl2* deficiency, we created a mouse with the complete coding region ablated (Fig. 1). As in several mouse models of gonadal diseases associated with haploinsufficiency in humans (13), lack of one copy of the single-exon gene resulted in no dramatic morphological or functional change. However, homozygous mutant mice experienced high rates of perinatal mortality (>50% died before 1 week, i.e. 26 out of 50), with a

*To whom correspondence should be addressed. Tel: +39 0706095668; Fax: +39 070503696; Email: pilia@unica.it
†The authors wish it to be known that, in their opinion, the first three authors should be regarded as joint First Authors.

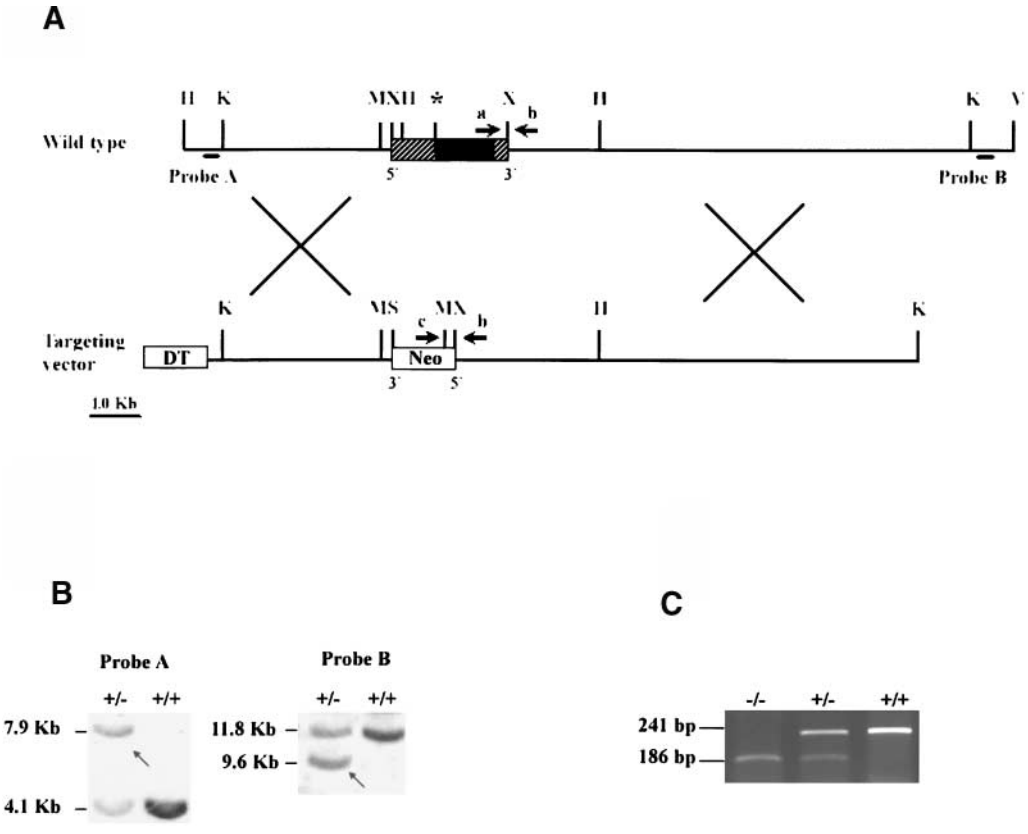

Figure 1. (**A**) Targeting construct and (**B**, **C**) genotyping. The structure of the 14 kb *Kpn*I (K) genomic DNA fragment containing the complete *Foxl2* gene is given in (A), where non-coding regions are indicated by hatchmarks, the coding region is in black and the start codon is indicated by an asterisk. Southern blot analysis of wild-type and homologous recombinant ES cells in (B) shows the wild-type clone (+/+) with the normal *Foxl2* allele band, while the targeted one (+/−) shows an additional band (arrow). PCR genotyping (C) gave the following amplicon size on mouse DNA: on wild-type, 241 bp; heterozygous, 241 and 186 bp; and homozygous, 186 bp.

1.7-fold male excess among survivors. In addition, like some BPES patients, *Foxl2* $^{-/-}$ animals were small (<85% the weight of wild-type littermates; *t*-test, $P < 0.05$), with the levels of serum IGF1, a major mediator of growth hormone function, reduced 60% (155–234 at 4 weeks versus 542–639 ng/ml in control littermates; *t*-test, $P < 0.05$). Craniofacial dysmorphic features comparable to BPES, particularly involving severe eyelid hypoplasia, were fully penetrant ($N = 82$) and were apparent by 13.5 dpc (Fig. 2A and B). Animals were born with open, necrotizing eyes (Fig. 2C–F). Comparable to BPES in humans, testis development was unaffected in heterozygous or homozygous *Foxl2*-null males. Heterozygous females were able to reproduce, though preliminary analyses indicated subfertility. Here we focus on patent ovarian anomalies in homozygous females.

Macroscopically, anomalies in *Foxl2* $^{-/-}$ female genitalia and gonads were evident by 2 weeks (fully penetrant, $N = 16$). Ovary size was reduced and tubes were hypotrophic with incomplete glandular cytodifferentiation, consistent with hypoestrogenism (Fig. 3, and data not shown). Earlier defects were manifest in histologic sections of 1-week ovaries ($N = 7$). In normal littermates at this stage we observed primordial and growing follicles up to the secondary stage [follicle stage 4 of (3)], characterized by the presence of two regular layers of cuboidal granulosa cells (Figs 4C and E and 5A and C). In contrast, in *Foxl2*-null females, the ovary was disorganized, as follows.

Growing oocytes were surrounded by granulosa-like epithelial cells assembled in a single layer (or occasionally in two layers over part of the oocyte surface). The epithelial cells were pleiomorphic, including a few flattened cells reminiscent of primordial follicles (Figs 4D and F and 5B and D). Some of these cells were positive for the proliferation marker Ki67 [expressed from late-G1 to M (14)], notably those located around growing oocytes [i.e. with diameter >20 μm (3,4)] (Fig. 5B). This indicates that although the program for granulosa cell differentiation and growth may have been induced to a partial extent, it was severely impaired from the earliest stages of folliculogenesis. These anomalies persisted, so that in contrast to wild-type mice, in which follicles with multiple layers of cuboidal granulosa cells were abundant by 2 weeks of life, mutant littermates had all oocytes still surrounded by one layer of granulosa cells ($N = 8$). At 8 weeks the anomalies were most conspicuous: granulosa-like cells surrounding growing oocytes were predominantly flattened and did not show mitotic activity by Ki67 staining (Fig. 5D). In addition, evidence for coordinated apoptosis of multiple adjacent granulosa cells, as observed in atretic follicles in the wild-type, was not found at any age in the mutant (as indicated by Tunel analysis; data not shown).

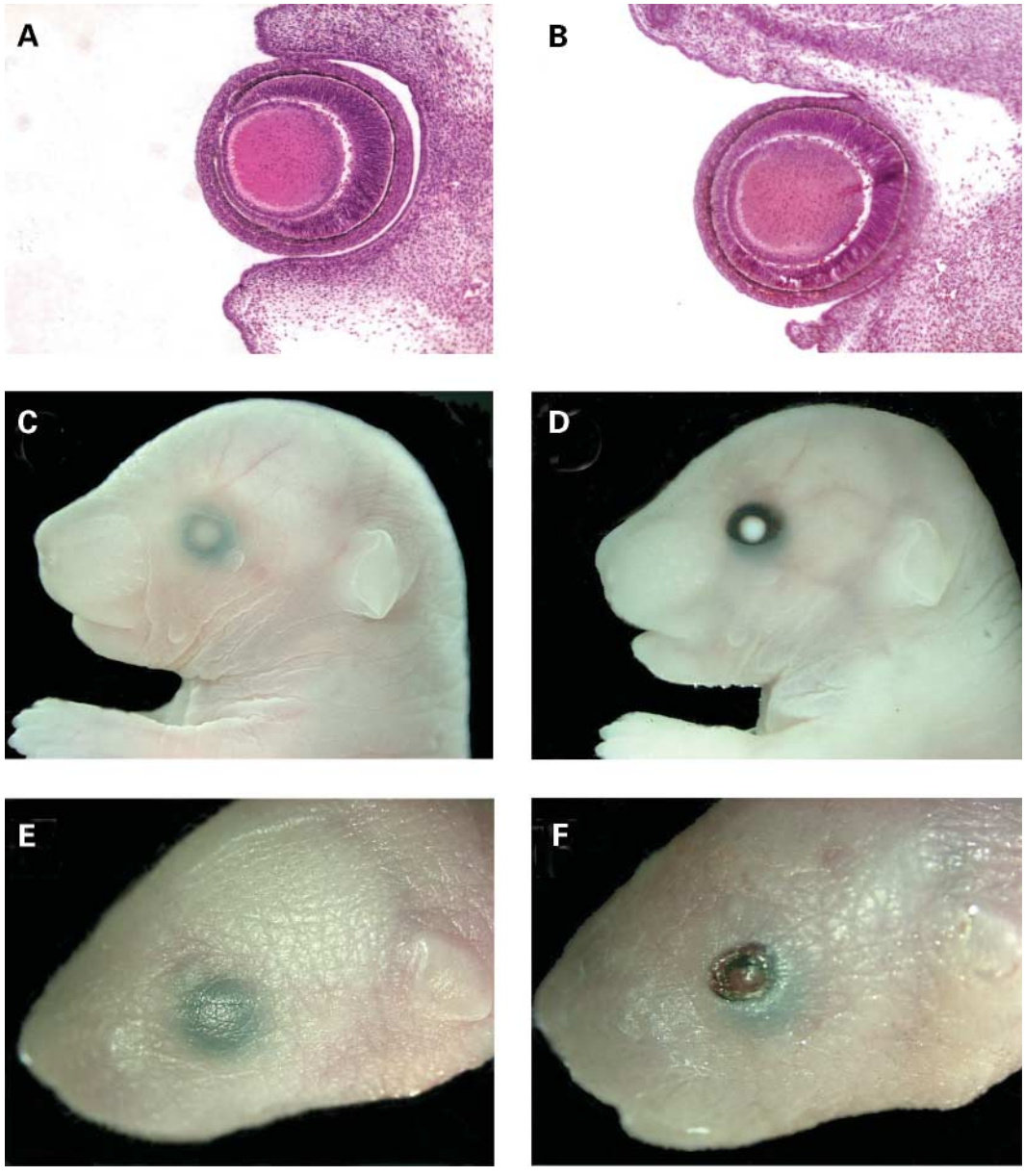

Figure 2. Eyelid anomalies. Defects are apparent in (**B**) 13.5 dpc *Foxl2*$^{-/-}$ embryos by histology with HE staining, correlated with overt eyelid hypoplasia and open eyes at (**D**) 17.5 dpc and (**F**) birth compared with (**A**, **C**, **E**) wild-type animals. Original magnification (C–F) 0.8×.

In spite of these anomalies in the somatic companion cells, oocyte differentiation was only partly affected, particularly at initial stages: a conspicuous zona pellucida was formed, and correspondingly, the levels of major oocyte regulators, *Gdf9* (15), c-*kit* (6) and *Fig-alpha* (8), were also indistinguishable from wild-type (Supplementary Material, Figs S1 and S2). Furthermore, ovarian morphology and oocyte counts at birth were similar to wild-type [$\sim$5000; $N = 12$; cf. (16)]. However, Figures 4–6 indicate that compared with wild-type, *Foxl2* $^{-/-}$ oocytes were growing at a slower rate at all ages. At 1 week, for example, the maximum diameter reached by oocytes was >10 μm smaller in mutant than in wild-type, and oocytes with a diameter >35 μm were $\sim$10-fold less abundant (Fisher's exact test, $P \ll 0.01$). Until 4 weeks, even the total number of oocytes recruited to growth, roughly assessed as those with a diameter >20 μm (3,4), appeared somewhat reduced in the knockout mice (Figs 4B and D, 5B and 6B and D). By 8 weeks, however, the wild-type ovary showed a range of oocyte sizes and follicle stages (predominantly primordial follicles with oocyte diameters <20 μm), while the oocytes in the mutant had almost all reached diameters >20 μm; they now occupied a large fraction of the ovary (Figs 4F and 6F), and many were undergoing apoptosis (data not shown). These data show that in the mutant essentially the entire cohort of oocytes were derepressed to grow between 4 and 8 weeks, though a defect may have been initiated earlier, if masked by the slower growth of the mutant oocytes.

Figure 3. Macroscopic appearance of tubes and ovaries. Pictures show organs at (**A**) birth, (**B**) 2 weeks, (**C**) 4 weeks, and (**D**) 8 weeks. The failure of growth in *Foxl2*$^{-/-}$ mice is apparent; (A–D) photographed with an MZFLIII Leica stereomicroscope. (A–C) homozygous *Foxl2*$^{-/-}$ on the right. (D) homozygous *Foxl2*$^{-/-}$ along with wild-type tubes and ovaries. Original magnification 0.8×.

The concurrence of early morphological anomalies associated with progressive alterations of oocyte growth and activation suggested a primary defect in follicle formation. This was supported by the following observations.

First, in the mutant, groups of up to at least 10 apposed oocytes, collectively surrounded by a layer of support cells, persisted for at least 8 weeks (Figs 4 and 6C–F). They correspond to oocyte clusters and to 'sex cords' (17) (i.e. oocytes, intercalated with pregranulosa cells, that would normally be progressively separated by interfollicular stroma). These structures were surrounded by basal lamina, staining for laminin-alpha-1 (18), and by stroma cells and arterioles, staining for smooth-muscle actin (18). At birth, these markers delineated prominent, branching cord-like configurations in both wild-type and mutant ovaries. Even at 8 weeks these structures in mutants had not given rise to individual follicles, whereas the process is essentially complete within 1 week in wild-type mice (Fig. 6, and data not shown).

Second, laminin-alpha-1 distribution was clearly abnormal from the time of primordial follicle formation (Fig. 6C–F): each follicle in normal ovaries was surrounded by a uniform immunostained layer, whereas mutant ovaries exhibited a layer of highly variable thickness, with apparent bifurcations and occasional abrupt termination in amorphous cellular masses.

These data show that *Foxl2* is required for primordial follicle formation, with a possible role in the synthesis of specialized basal lamina. In addition, we failed to detect steroidogenic cells in *Foxl2*$^{-/-}$ mutants, as assayed by immunostaining with cytochrome P450 side-chain cleavage enzyme (19), the rate-limiting enzyme in the pathway from cholesterol to steroids (Fig. 7A and B). Thus, in the absence of Foxl2, several cell lineages were not induced—including

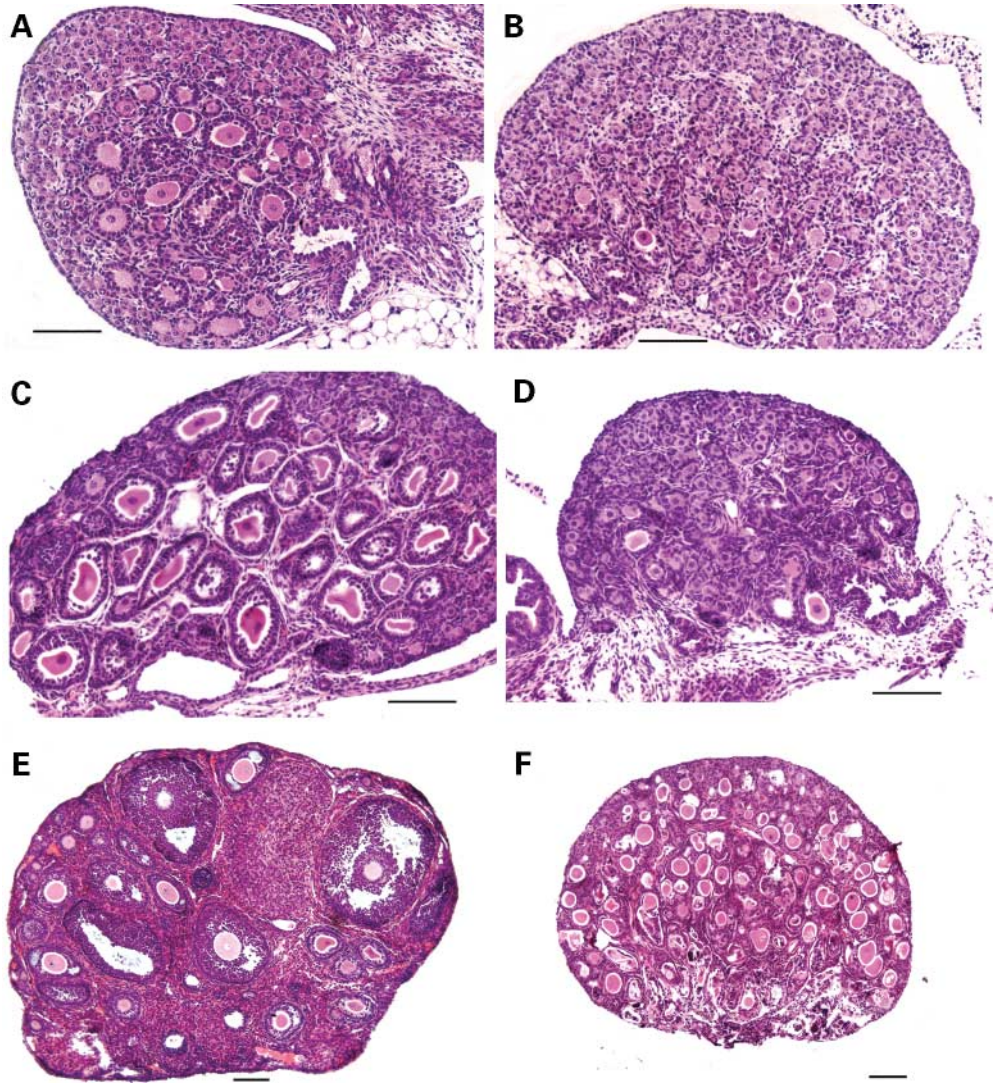

Figure 4. Morphological appearance by HE staining of ovary sections. Compared with (**A**, **C**, **E**) wild-type littermates, (**B**, **D**, **F**) knockout mice show slower oocyte growth (smaller average oocyte diameter) at (B, D) 1 and 2 weeks, and far greater abundance of growing oocytes at (F) 8 weeks. Somatic cells appear disorganized in the knockout, with mainly one layer of epithelial cells observed around (B, D, F) growing oocytes and reduced stroma. Bars: 100 μm.

ovarian steroidogenic theca cells and [unlike models like *Gdf9*-null mice (20)] interstitial glands. In contrast, the low-affinity nerve growth factor receptor, NGFR/p75, a marker of newborn gonadal stroma (21), was subsequently downregulated in control littermates but persisted in delimited regions of mutant ovaries (Fig. 7C and D). These data indicate the persistence of primitive stroma, which is seemingly 'frozen' in a newborn state in the *Foxl2*$^{-/-}$ ovaries.

The expression pattern of Foxl2 provided further information about the timing and cell-types involved in the anomalies. A specific polyclonal antibody detected Foxl2 in somatic cells of the fetal ovary and, at decreasing levels, in granulosa cells of adult follicles from the primordial to the preantral stage (data not shown), consistent with previous studies of RNA and protein expression [(22) and references therein]. More importantly, in the neonatal wild-type ovary (Fig. 8), Foxl2 expression was clearly observed in pregranulosa cell nuclei. Many Foxl2-positive nuclei were immediately apposed to oocytes and intercalated amidst the nascent follicles. All Foxl2-positive cells were ki67-negative (14) (non-dividing), and some expressed the epithelial marker (23) cytokeratin-18 (Fig. 8C and D). Furthermore, the most external Foxl2-positive cells were oriented perpendicular to the surface of the ovary, with an external pole adjacent to Foxl2-negative, ki67-positive (dividing) round nuclei of surface epithelial cells (Fig. 8D). Ovarian surface epithelium is an important source of granulosa cells, which do not multiply while they migrate to reach the oocytes and form the primordial follicles (1–4,24). This is consistent with Foxl2 expressed in pregranulosa cells from their earliest involvement in histogenesis. Granulosa cell blockage at the prefollicle stage likely explains the persistence of primitive stroma (Fig. 7), though low expression of Foxl2 in a few stroma cells has not been excluded completely.

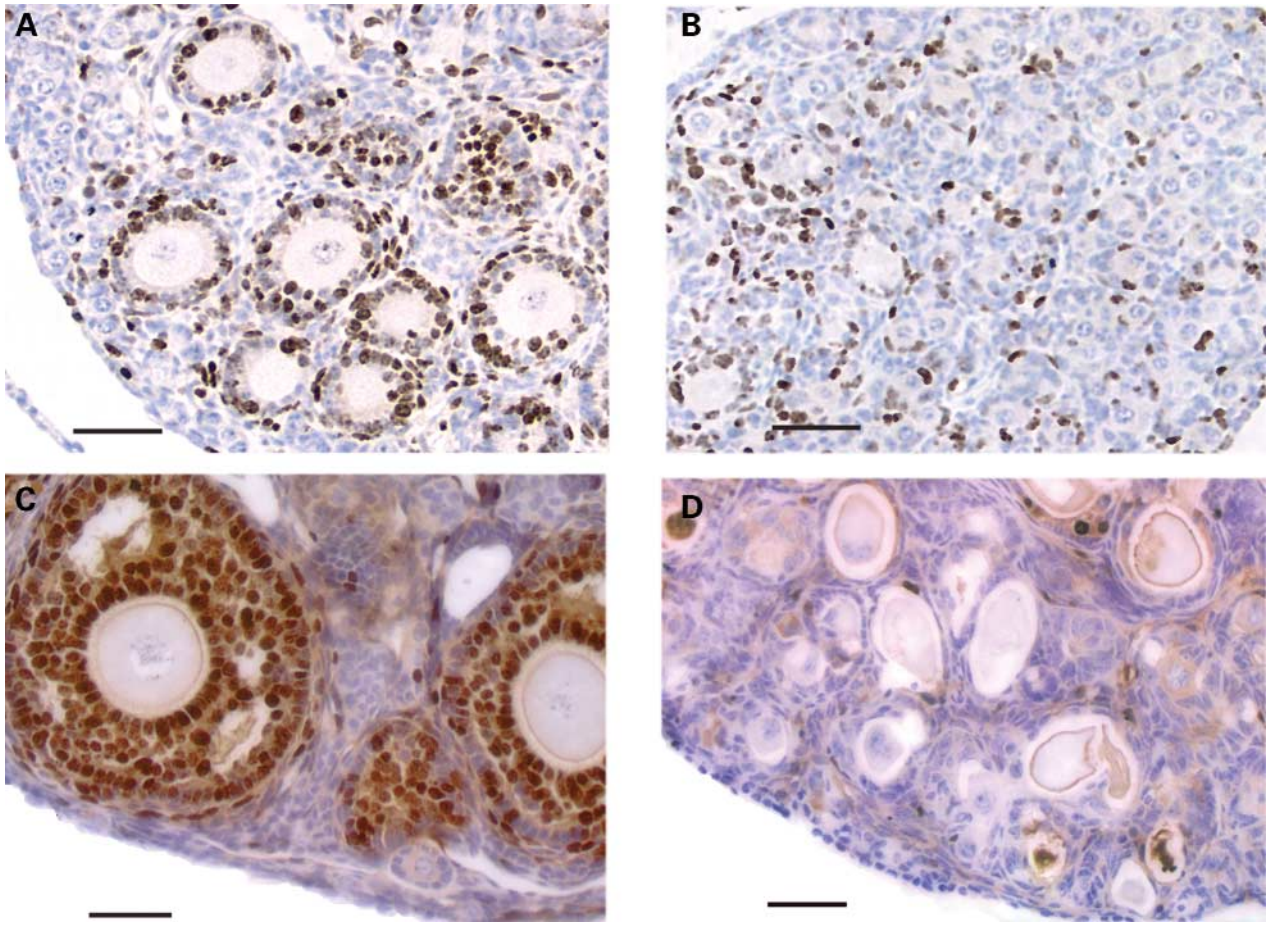

Figure 5. Immunohistochemistry detecting proliferation marker Ki67. Reduction or absence of multiplication in the epithelial cell compartment is observed in the (**B**, **D**) mutant ovary compared with (**A**, **C**) wild-type littermates at 1 and 8 weeks post-natal. Bars: 50 μm.

DISCUSSION

We recently isolated *FOXL2*, encoding a FOX winged-helix forkhead gene transcription factor, as a gene mutated in patients with BPES (12). The severity of the anomalies being confined to essentially two organs in this syndrome (eyelids and ovary) and the selective expression of the gene largely in those two organs suggested to us that the underlying gene, *FOXL2*, might control highly specific mechanisms with pervasive effects in development. Thus its functional characterization in mice was likely to complement the large body of knowledge on ovary formation and maturation. Here, we show first that *Foxl2*$^{-/-}$ mice exhibit defects comparable to BPES in humans, thereby providing an entry point to study major features of this human condition. Second, this mouse model can be relevant for human POF in general, because it controls a developmental process (histogenesis) that is pivotal to ovarian reproductive competence. Third, the initial analysis presented here indicates that *Foxl2*, expressed in granulosa cell precursors, regulates the fate of all major ovarian cell lineages, including oocytes and stroma. A central role of pregranulosa cells in regulating oocyte and stroma growth and differentiation might then be comparable to the critical function of Sertoli cell precursors in the embryonic testis (25).

Extra-ovarian phenotypes in the knockout mice affect systems that have been less characterized, but the defects observed are likely to be segmental: the failure of eyelid formation correlated with the lack of expression of *Foxl2* in the periorbital mesenchyme (12), and the smaller size possibly correlated with the lack of expression in the pituitary (26). For ovarian development, however, where studies have generally been more extensive, it is notable that the defects observed occur at an earlier step than seen in null mutants for several previously identified regulatory genes. Those genes preferentially control growth [e.g. *Gdf9* (15,20), *Fshr* (27)] or recruitment [*Foxo3a* (28)] of primordial follicles that are competent to mature, and steroidogenically active stroma forms even in their absence.

In a recently reported *Foxl2*$^{-/-}$ mouse model (29), extensive expression of Gdf9 was observed, as seen in oocytes here as well (Supplementary Material Fig. S1). This was interpreted as indicating an early derepression of oocyte growth, leading to the inference that *Foxl2* might be required to simultaneously repress oocyte activation and somehow also promote follicle growth. However, the additional histologic anomalies studied here indicate that in the absence of *Foxl2*, complete individual follicles segregated by stroma never form, with massive oocyte growth occurring relatively later. Further studies should determine more precisely the timing and

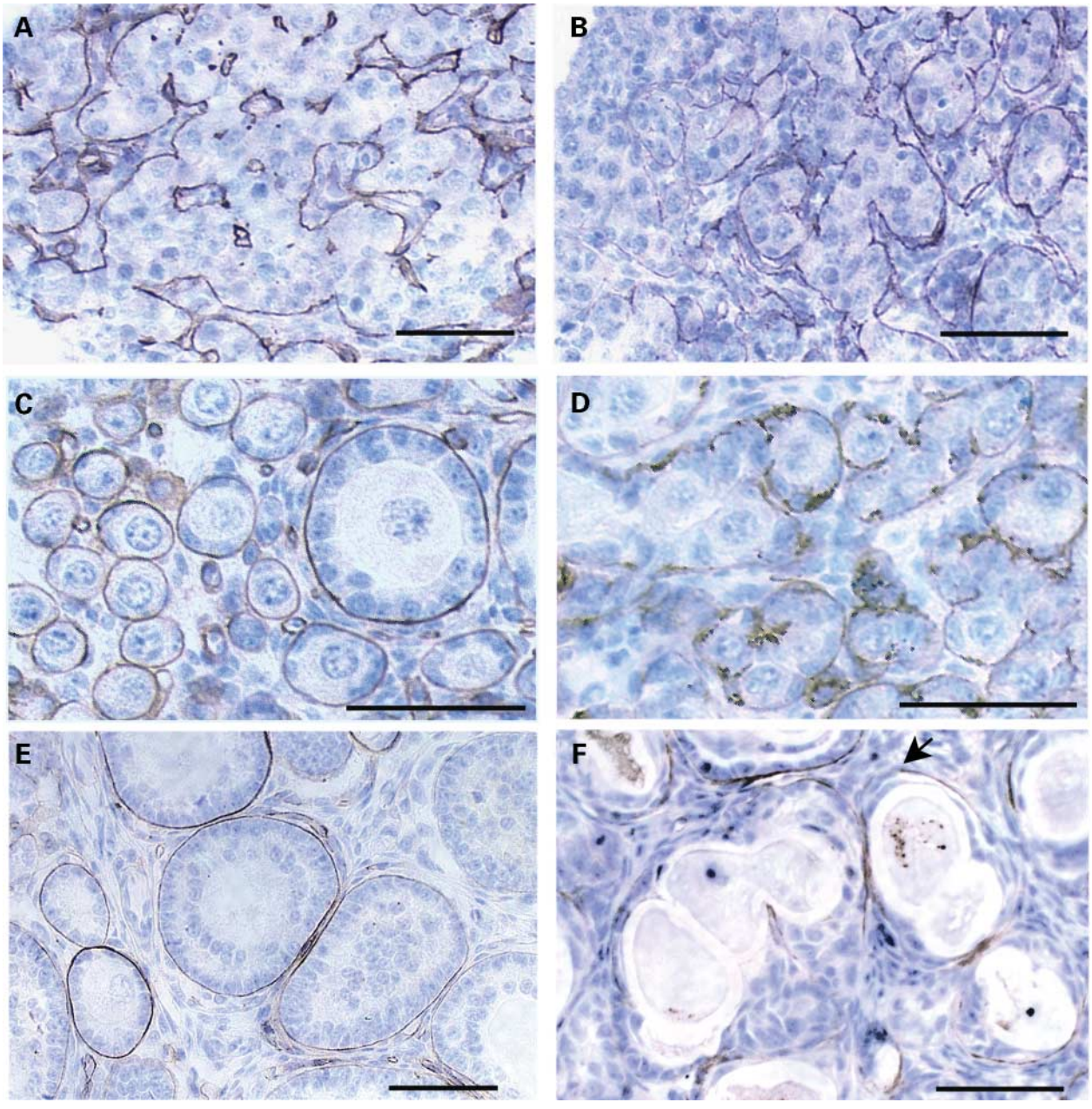

Figure 6. Distribution of laminin-alpha-1 by immunohistochemistry. Immunostaining of mouse ovarian sections at (**A**, **B**) birth, (**C**, **D**) 1 week and (**E**, **F**) 8 weeks. Anomalies are obvious in *Foxl2*-null mice by 1 week. Staining shows a continuous regular basal layer around individual follicles at various stages of maturation in (C, E) the wild-type littermate compared to an apparently fragmentary layer of variable thickness in the (D, F) *Foxl2* knockout. Arrow: truncation of a layer. Bars: 50 μm.

pattern of oocyte anomalies; but the concurrence of pervasive disruption of follicle formation and deregulated oocyte growth (whether immediate or delayed) strongly supports the long-held view that organization of ovary architecture is essential to establish the pool of functional oocytes (3,4,17,24,30), and indicates a central coordinating function for *Foxl2*.

In other known mouse mutations classified as growth defects, occasional unseparated oocyte doublets have been observed; however, in spite of the recognized role of basal lamina in other developmental systems (18), lamina defects have customarily not been investigated. Taken together, our data indicate that ovarian failure associated with BPES results primarily from the failure of granulosa cells in follicle formation, leading to deregulated oogenesis by an unknown mechanism that requires further analyses. Investigating ovarian morphogenetic defects in the polled-intersex goat, thought to be equivalent to BPES and involving *Foxl2* down-regulation (31), may help understand sex reversal in that case; but *Foxl2* $^{-/-}$ mice should particularly facilitate the analysis of primordial follicle morphogenesis uncoupled from sex determination. This knockout mouse provides the first model directly relevant to ovarian gonadal dysgenesis in humans,

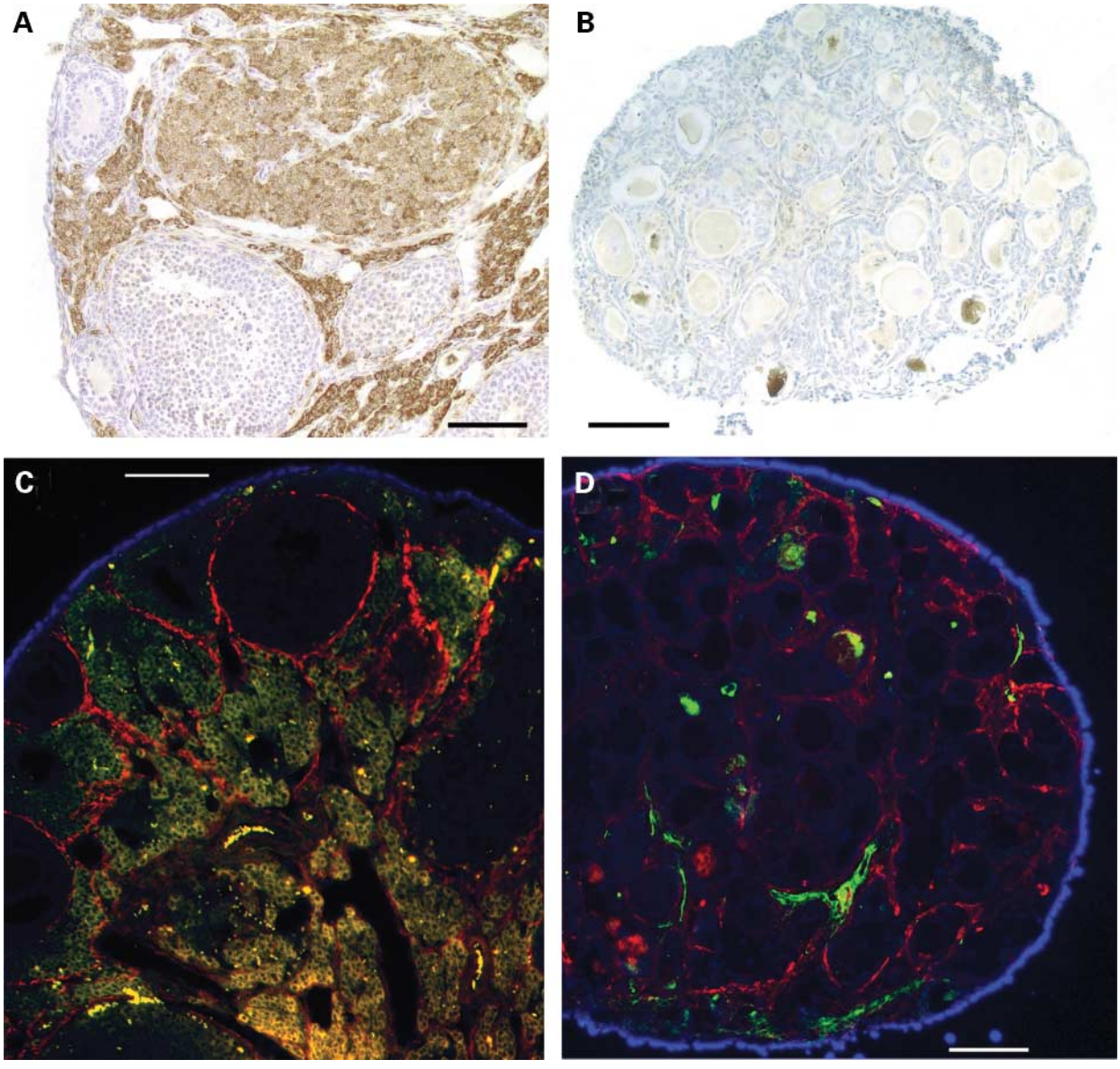

Figure 7. Stromal defects at 8 weeks in *Foxl2*$^{-/-}$ mice. P450ssc expression (immunoperoxidase DAB staining with hematoxylin counterstaining) is extensive in interstitial glands, theca, and luteal cells in sections of (**A**) wild-type littermate, but no specific staining is detected in (**B**) *Foxl2*$^{-/-}$. Double staining of smooth-muscle actin (red) and NGFR/p75 (green) shows a comparable level of expression of smooth-muscle actin in (**C**) wild-type littermate and (**D**) knockout ovary; whereas NGFR/p75 shows defined interstitial areas with strong expression (green) in sections from (D) *Foxl2*$^{-/-}$, whereas the wild-type has background levels of expression (yellow). Bars: 100 μm.

along with a route to genes selectively involved in the determination of the initial follicle pool. Such genes should include candidates for mutation in instances of POF without extra-ovarian anomalies, where affected genes have been difficult to identify [(5,32) and references therein]. In the long run, they may provide targets for therapeutic intervention.

MATERIALS AND METHODS

Knockout mice

We sequenced the genomic region (33) and replaced a 2.177 kb *Foxl2*-containing *Xho*I–*Xho*I fragment using a targeting vector (Fig. 1A) with diphtheria toxin negative selection and neomycin resistance (Neo) positive selection. A 14 kb *Kpn*I (K) genomic DNA fragment from the RPCI-21 (129S6/SvEvTac) mouse PAC library containing the complete *Foxl2* gene was cloned into a pBS KS^{+} hosting the diphtheria toxin gene as a negative selection marker. A 2.177 kb *Xho*I fragment including the entire *Foxl2* coding region was replaced with a 1.157 kb *Sal*I (S)–*Xho*I (X) Neo gene cassette. After electroporation, 170 Neo-resistant 129SV/Tac embryonic stem cell transformant clones were isolated. Southern analysis (Fig. 1B) identified three clones with *Foxl2* replaced. Two were microinjected into 10 blastocysts each to give three and four chimeras, respectively (inGenious Targeting Laboratory, Inc., NY, USA). *Foxl2*$^{+/-}$

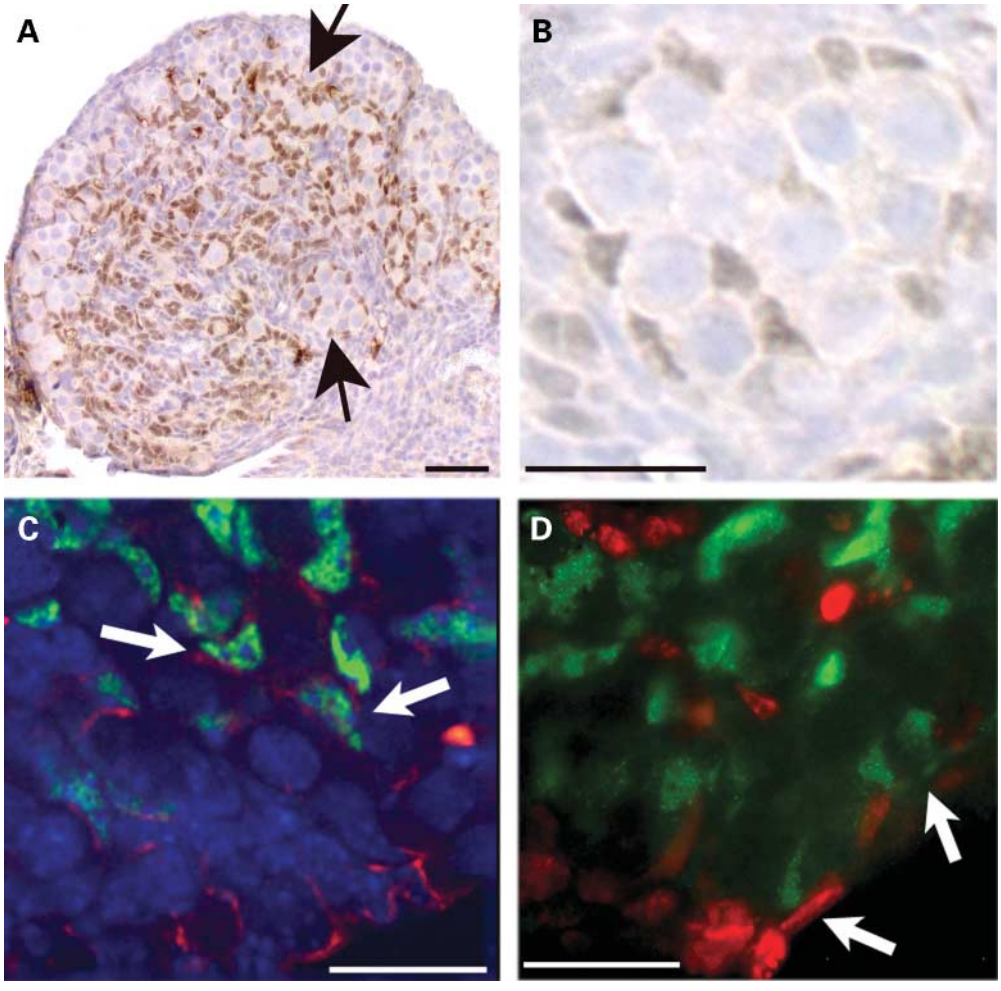

Figure 8. Expression of *Foxl2* in 3-day-old mice. Immunohistochemistry with anti-Foxl2 antibody. (**A**) Expression (immunoperoxidase DAB staining brown with hematoxylin counterstaining) in pregranulosa cell nuclei during the production of primordial follicles. Arrows indicate intercalation of pregranulosa cells within oocyte clusters. (**B**) Higher magnification of (A), showing an oocyte cluster with partly intercalated Foxl2-positive nuclei. (**C**) Double staining for Foxl2 (green) and cytokeratin-18 (red) (blue: DAPI counterstaining). Cytokeratin-18 staining near or at the surface of the ovary, with Foxl2 internal. Some cells express both markers (arrows). (**D**) Double staining for Foxl2 (green) and the proliferation marker Ki67 (red). Foxl2-expressing cells are non-proliferating, with some near the ovary surface (arrows; see text). Bars: (A) 50 μm and (B–D) 20 μm.

mutant mice were bred to C57/B6 (Jackson Laboratory), NIHS-BC, and 129S6/SvEvTac (Taconic) mice. Heterozygous offspring were bred to generate the *Foxl2*$^{-/-}$ mice studied and tail DNA genotyping performed by PCR (Fig. 1C). For Southern-blot analysis of wild-type and homologous recombinant ES cells, DNA was digested with *Hin*dIII (H) (Fig. 1B, left panel) and *Vsp*nI (V)–*Mlu*I (M) (Fig. 1B, right panel; the locations of the sites are indicated in Fig. 1A) and hybridized with probe A (a 652 bp PCR fragment amplified by primer forward AGGAAAGTGGCAGTGTGCAG and reverse GG CTCTGGTGTTTTGCTTGG) and probe B (a 709 bp PCR fragment amplified by primer forward TACCCTCTACCACCT CCTT and reverse GAACTAGGCAAACACACCAATG). PCR reactions (Fig. 1C) detected the wild-type and mutant alleles with one common primer (b: GGATCTCTGAGTGCCAACGC) and a second primer recognized the wild-type sequence (a: CACGGGAAAGCAGAGGCCGC) or the replacement Neo cassette sequence (c: CACACTGCTCGACATTGGGTG). PCR reactions were performed twice, i.e. both in a multiplex PCR reaction and separately for the two alleles. Mice were euthanized ethically according to ACUC-approved NIA Animal Protocol 1218-03. Serum IGF1 levels were measured by solid-phase RIA (Anilytics, Gaithersburg, MD, USA).

Histology and morphometry

Embryos and organs of different ages (13.5 dpc, 17.5 dpc, P1, P7, P14, 4 weeks and 8 weeks) were fixed in 4% paraformaldehyde or Histochoice® (Amresco, Solon, OH, USA), embedded in paraffin, serially sectioned at 5 μm, and stained with hematoxylin–eosin (HE) or processed for immunohistochemistry or RNA *in situ* hybridization. Images in Figure 2C–F were taken with an MZFLIII Leica stereomicroscope. Images in Figure 8C and D were taken with a HiRes CCD camera and processed on a Deltavision system version 5.10. All other images were taken with an Axiovert

200 microscope (Zeiss, Gottingen, Germany) coupled to a Spot® camera (Diagnostic Instruments, Sterling Heights, MI, USA) and processed with Adobe Photoshop® version 7.0. Morphometric analysis (34) was assisted by ImageJ software (www.rsb.inf.nih.gov).

Immunohistochemistry

Antibodies used were alpha-laminin (mab1905), cytokeratin-18 (cbl177), NGFR/p75 (ab1554), smooth-muscle actin (Cbl171) (Chemicon, Temecula, CA, USA); P450ssc (P450SCCabr) (Research Diagnostics, Flanders, NJ, USA); Ki67 (BD-550609) (Pharmingen, San Diego, CA, USA); c-kit (sc-168) (Santa-Cruz Biotechnology, Santa Cruz, CA, USA). Immunoperoxidase staining was with the biotin/streptavidin-based LSAB2 system (Dako); immunofluorescent secondary antibodies were purchased from Molecular Probes (Eugene, OR, USA). Rabbit polyclonal anti-Foxl2 was raised against residues FRPPPAHFQPGKGLF and DHDSKTGALHSRLDL (Eurogentec s.a., Belgium) and used after affinity purification; specificity was confirmed by western blotting. Tunel assays used Roche (Nutley, NJ, USA) kit 1684817.

RNA *in situ* hybridization

Mouse *in situ* hybridization was performed on paraffin sections with digoxygenin-labeled RNA probes according to conventional techniques. *Fig-alpha* probe was transcribed from a PCR amplicon covering nucleotide 188 to 627 (GenBank accession U91840) cloned into Pcr4topo (Invitrogen, Carlsbad, CA, USA). *Gdf9* probe was from a construct of the NIA cDNA library (GenBank accession BG080778).

SUPPLEMENTARY MATERIAL

Supplementary Material is available at HMG Online.

ACKNOWLEDGEMENTS

We thank Minoru Ko for critical suggestions, Lioudmila Sharova for indispensable help with ES cultures, Mara Marongiu for assistance in the antibody purification, and Telethon service for screening of mouse BAC clones. Work was supported by Telethon grant no. GP0049Y01 to L.C. and Assessorato Igiene e Sanità, Legge Regionale n.11 del 30.04.1990.

REFERENCES

1. Hirshfield, A.N. (1991) Development of follicles in the mammalian ovary. *Int. Rev. Cytol.*, **124**, 43–101.
2. Zuckermann, S. (1951) The numbers of oocytes in the mature ovary. *Rec. Prog. Horm. Res.*, **6**, 63–109.
3. Peters, H. (1969) The development of the mouse ovary from birth to maturity. *Acta Endocrinol.*, **62**, 98–116.
4. Byskov, A.G. (1986) Differentiation of mammalian embryonic gonad. *Physiol. Rev.*, **66**, 71–117.
5. Simpson, J.L. and Rajkovic, A. (1999) Ovarian differentiation and gonadal failure. *Am. J. Med. Genet.*, **89**, 186–200.
6. Williams, D.E., de Vries, P., Namen, A.E., Widmer, M.B. and Lyman, S.D. (1992) The steel factor. *Dev. Biol.*, **151**, 368–376.
7. Duncan, M., Cummings, L. and Chada, K. (1993) Germ cell deficient (gcd) mouse as a model of premature ovarian failure. *Biol. Reprod.*, **49**, 221–227.
8. Soyal, S.M., Amleh, A. and Dean, J. (2000) FIGalpha, a germ cell-specific transcription factor required for ovarian follicle formation. *Development*, **127**, 4645–4654.
9. Vainio, S., Heikkila, M., Kispert, A., Chin, N. and McMahon, A.P. (1999) Female development in mammals is regulated by Wnt-4 signalling. *Nature*, **397**, 405–409.
10. Spears, N., Molinek, M.D., Robinson, L.L., Fulton, N., Cameron, H., Shimoda, K., Telfer, E.E., Anderson, R.A. and Price, D.J. (2003) The role of neurotrophin receptors in female germ-cell survival in mouse and human. *Development*, **130**, 5481–5491.
11. Elvin, J.A. and Matzuk, M.M. (1998) Mouse models of ovarian failure. *Rev. Reprod.*, **3**, 183–195.
12. Crisponi, L., Deiana, M., Loi, A., Chiappe, F., Uda, M., Amati, P., Bisceglia, L., Zelante, L., Nagaraja, R., Porcu, S. *et al.* (2001) The putative forkhead transcription factor FOXL2 is mutated in blepharophimosis/ptosis/epicanthus inversus syndrome. *Nat. Genet.*, **27**, 159–166.
13. Capel, B. (1998) Sex in the 90s: SRY and the switch to the male pathway. *Annu. Rev. Physiol.*, **60**, 497–523.
14. Yu, C.C., Woods, A.L. and Levison, D.A. (1992) The assessment of cellular proliferation by immunohistochemistry: a review of currently available methods and their applications. *Histochem. J.*, **24**, 121–131.
15. Dong, J., Albertini, D.F., Nishimori, K., Kumar, T.R., Lu, N. and Matzuk, M.M. (1996) Growth differentiation factor-9 is required during early ovarian folliculogenesis. *Nature*, **383**, 531–535.
16. Canning, J., Takai, Y. and Tilly, J.L. (2003) Evidence for genetic modifiers of ovarian follicular endowment and development from studies of five inbred mouse strains. *Endocrinology*, **144**, 9–12.
17. Merchant-Larios, H. and Chimal-Monroy, J. (1989) The ontogeny of primordial follicles in the mouse ovary. *Prog. Clin. Biol. Res.*, **296**, 55–63.
18. Rodgers, R.J., Irving-Rodgers, H.F. and Russell, D.L. (2003) Extracellular matrix of the developing ovarian follicle. *Reproduction*, **126**, 415–424.
19. Simpson, E.R. (1979) Cholesterol side-chain cleavage, cytochrome P450, and the control of steroidogenesis. *Mol. Cell. Endocrinol.* **13**, 213–227.
20. Elvin, A., Yan, C., Wang, P., Nishimori, K. and Matzuk, M.M. (1999) Molecular characterization of the follicle defects in the growth differentiation factor 9-deficient ovary. *Mol. Endocrinol.*, **13**, 1018–1034.
21. Dissen, G.A., Hirshfield, A.N., Malamed, S. and Ojeda, S.R. (1995) Expression of neurotrophins and their receptors in the mammalian ovary is developmentally regulated: changes at the time of folliculogenesis. *Endocrinology*, **136**, 4681–4692.
22. Loffler, K.A., Zarkower, D. and Koopman, P. (2003) Etiology of ovarian failure in blepharophimosis ptosis epicanthus inversus syndrome: FOXL2 is a conserved, early-acting gene in vertebrate ovarian development. *Endocrinology*, **144**, 3237–3243.
23. Appert, A., Fridmacher, V., Locquet, O. and Magre, S. (1998) Patterns of keratins 8, 18 and 19 during gonadal differentiation in the mouse: sex- and time-dependent expression of keratin 19. *Differentiation*, **63**, 273–284.
24. Rajah, R., Glaser, E.M. and Hirshfield, A.N. (1992) The changing architecture of the neonatal rat ovary during histogenesis. *Dev. Dyn.*, **194**, 177–192.
25. McLaren, A. (1991) Development of the mammalian gonad: the fate of the supporting cell lineage. *Bioessays*, **13**, 151–156.
26. Kioussi, C., O'Connell, S., St-Onge, L., Treier, M., Gleiberman, AS., Gruss, P. and Rosenfeld, MG. (1999) Pax6 is essential for establishing ventral–dorsal cell boundaries in pituitary gland development. *Proc. Natl Acad. Sci. USA*, **96**, 14378–14382.
27. Aittomaki, K., Lucena, J.L., Pakarinen, P., Sistonen, P., Tapanainen, J., Gromoll, J., Kaskikari, R., Sankila, E.M., Lehvaslaiho, H., Engel, A.R. *et al.* (1995) Mutation in the follicle-stimulating hormone receptor gene causes hereditary hypergonadotropic ovarian failure. *Cell*, **82**, 959–968.
28. Castrillon, D.H., Miao, L., Kollipara, R., Horner, J.W. and DePinho, R.A. (2003) Suppression of ovarian follicle activation in mice by the transcription factor Foxo3a. *Science*, **301**, 215–218.

29. Schmidt, D. Ovitt, C.E., Anlag, K., Fehsenfeld, S., Gredsted, L., Treier, A.C. and Treier, M. (2004) The murine winged-helix transcription factor Foxl2 is required for granulosa cell differentiation and ovary maintenance. *Development*, **131**, 933–942.
30. Byskov, A.G., Guoliang, X. and Andersen, C.Y. (1997) The cortex–medulla oocyte growth pattern is organized during fetal life: an *in-vitro* study of the mouse ovary. *Mol. Hum. Reprod.*, **3**, 795–800.
31. Pailhoux, E., Vigier, B., Chaffaux, S., Servel, N., Taourit, S., Furet, J.P., Fellous, M., Grosclaude, F., Cribiu, E.P., Cotinot, C. and Vaiman, D.A. (2001) 11.7-kb Deletion triggers intersexuality and polledness in goats. *Nat. Genet.*, **29**, 453–458.
32. Harris, S.E., Chand, A.L., Winship, I.M., Gersak, K., Aittomaki, K. and Shelling, A.N. (2002) Identification of novel mutations in FOXL2 associated with premature ovarian failure. *Mol. Hum. Reprod.*, **8**, 729–733.
33. Crisponi, L. Uda, M., Dieana, M., Loi, A., Nagaraja, R., Chiappe, F., Schlessinger, D., Cao, A. and Pilia, G. (2004) *FOXL2* inactivation by a translocation 171 kb away: analysis of 500 kb of chromosome 3 for candidate long-range regulatory sequences. *Genomics*, **83**, 757–764.
34. Baker, T.G. (1963) A quantitative and cytological study of germ cells in human ovaries. *Proc. R. Soc. Lond. B. Biol. Sci.*, **158**, 417–433.